

## Hydrolysis and ion exchange of titania nanoparticles towards large-scale titania and titanate nanobelts for gas sensing applications

This article has been downloaded from IOPscience. Please scroll down to see the full text article.

2010 J. Phys. D: Appl. Phys. 43 035401

(<http://iopscience.iop.org/0022-3727/43/3/035401>)

[The Table of Contents](#) and [more related content](#) is available

Download details:

IP Address: 137.132.123.69

The article was downloaded on 05/02/2010 at 00:58

Please note that [terms and conditions apply](#).

# Hydrolysis and ion exchange of titania nanoparticles towards large-scale titania and titanate nanobelts for gas sensing applications

Somaiah Bela<sup>1</sup>, Andrew See Weng Wong<sup>2</sup> and Ghim Wei Ho<sup>1,3</sup>

<sup>1</sup> Department of Electrical and Computer Engineering, National University of Singapore, 4 Engineering Drive, Singapore 117576, Singapore

<sup>2</sup> Institute of Materials Research and Engineering, 3 Research Link, Singapore 117602, Singapore

E-mail: [elehgw@nus.edu.sg](mailto:elehgw@nus.edu.sg)

Received 2 July 2009, in final form 11 November 2009

Published 8 January 2010

Online at [stacks.iop.org/JPhysD/43/035401](http://stacks.iop.org/JPhysD/43/035401)

## Abstract

One-dimensional titanate and titania nanostructures are prepared by hydrothermal method from titania nanoparticles precursor via hydrolysis and ion exchange processes. The formation mechanism and the reaction process of the nanobelts are elucidated. The effects of the NaOH concentration, HCl leaching duration and the calcination temperature on the morphology and chemical composition of the produced nanobelts are investigated. Na<sup>+</sup> ions of the titanate nanobelts can be effectively removed by longer acid leaching and neutralization process and transformed into metastable hydrogen titanate compound. A hybrid hydrogen titanate and anatase titania nanobelts can be obtained under dehydration process of 500 °C. The nanobelts are produced in gram quantities and easily made into nanostructure paper for the bulk study on their electrical and sensing properties. The sensing properties of the nanobelts sheet are tested and exhibited response to H<sub>2</sub> gas.

(Some figures in this article are in colour only in the electronic version)

## 1. Introduction

There is a great interest in the development of titanates and titania-based solids with nanoscale dimensions and specific morphology such as nanoparticles, nanowires/nanorods and nanotubes depending on the applications. These high-surface-to-volume titanate and titania nanostructures have many promising photoelectrical [1, 2], biomedical [3] and storage properties [4–7]. Titanates are well-known functional ceramic materials with dielectric, piezoelectric, ferroelectric and low absorption of infrared radiation properties [8] while titania is often used as pigments, photocatalysts for degrading organic pollutants under ultraviolet irradiation [9, 10], photoactive materials for solar cell [11, 12], gas sensing [13] and Li ion battery materials [14, 15]. As a result of the wide range of valuable functional properties associated with these materials, it is important to develop simple and inexpensive strategies for

large-scale synthesis which can control the morphology and chemical composition of titanate and titania nanostructures.

Titanate and titania nanostructures have been prepared and investigated by several groups [8, 16, 17]. The chemical and physical properties of titanates and titania nanostructures depend on the method of preparation as well as precursor and reaction parameters used Peng *et al* have synthesized titania nanotubes using anatase TiO<sub>2</sub> particles by the hydrolysis of titanium tetrabutoxide in butyl alcohol solution [16]. The bundle-like structure of titania nanotubes was synthesized with anatase TiO<sub>2</sub> particles mixed with NaOH aqueous solution in an autoclave vessel maintained at 210 °C for 24 h. The precipitate after hydrothermal treatment was washed with deionized (DI) water, dried under vacuum for 10 h and calcined at 500 °C for 1 h to produce titania nanotubes. Similarly, solution-based synthetic method based on TiO<sub>2</sub> nanoparticles and NaOH was employed to produce a large scale of ribbon-like titanates [17]. The resulting suspension

<sup>3</sup> Author to whom any correspondence should be addressed.

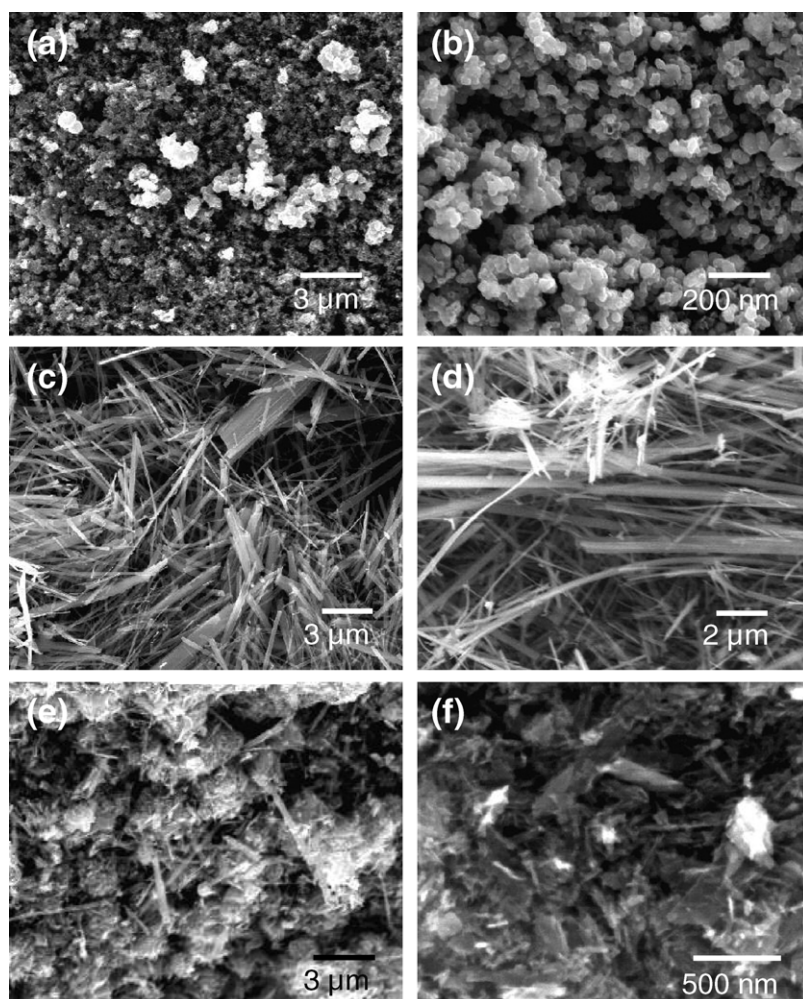


**Figure 1.** SEM images nanobelts synthesized with various NaOH concentrations of (a)–(b) 5M, (c)–(d) 10M and (e)–(f) 15M.

of  $\text{TiO}_2$  nanoparticles in NaOH was heated at 160–180 °C for 48 h. The resulting white precipitate was filtered, washed and dried in vacuum at 60 °C for 3 h to produce sodium titanates ( $\text{Na}_2\text{Ti}_3\text{O}_7$ ) nanobelts. Another way to produce titanate nanowires is prepared via a hydrothermal reaction between an inorganic titanium salt,  $\text{TiOSO}_4\cdot\text{H}_2\text{O}$  and concentrated NaOH solution [8]. The hydrolysis was carried out at 200 °C for 48 h to yield titanate precipitates. All these methods produce sodium titanate nanostructures since high temperature heat treatment is not carried out to transform the titanates into  $\text{TiO}_2$  polymorphs (anatase and rutile phase) [8, 17].

Though to date many synthesis methods for preparing titania and titanate nanostructures have been reported, very little literature has revealed the control of alkali hydrolysis and acid ion exchange concentration and duration to produce hybrid titanate and titania nanobelts in a large-scale quantity for gas sensing applications. In this study, titania and titanate nanobelts are synthesized from  $\text{TiO}_2$  powder based on hydrolysis and ion exchange of NaOH base and HCl acid, respectively. The effects of the NaOH concentration, HCl acid washing duration and the calcination temperature on the morphology and chemical composition of the produced nanobelts are investigated. In addition, the formation mechanism and the reaction process of the nanobelts are

elucidated. The nanobelts are produced in gram quantities and easily made into nanostructured paper sheet for the study of electrical and sensing properties. It is noted that successful synthesis of titanate and titania nanobelts in a large scale will open up the possibilities of rational study and applications of the physical and chemical properties of Ti–O nanomaterial systems in bulk quantities.

## 2. Experimental section

0.1 g titanium (IV) oxide was added to 20 ml of 10M NaOH aqueous solution and mixed well. The solution was then heated to 200 °C in a Teflon-lined autoclave for 2 days. The cooled product was washed thoroughly. This was done by adding DI water to the sample, centrifuging and then decanting the liquid several times. The white precipitate was then left to dry before immersing in 10 ml of 0.1M aqueous solution of HCl for different durations of 24 up to 72 h. The product was then washed thoroughly and annealed at various temperatures of 250 and 500 °C in a ceramic crucible for 1 h.

0.04 g of the as-synthesized nanobelts was dispersed in 200 ml of DI water to make into nanobelts sheet. The thickness of the nanostructures sheet can be tuned according to the amount of nanostructures used. The nanostructures

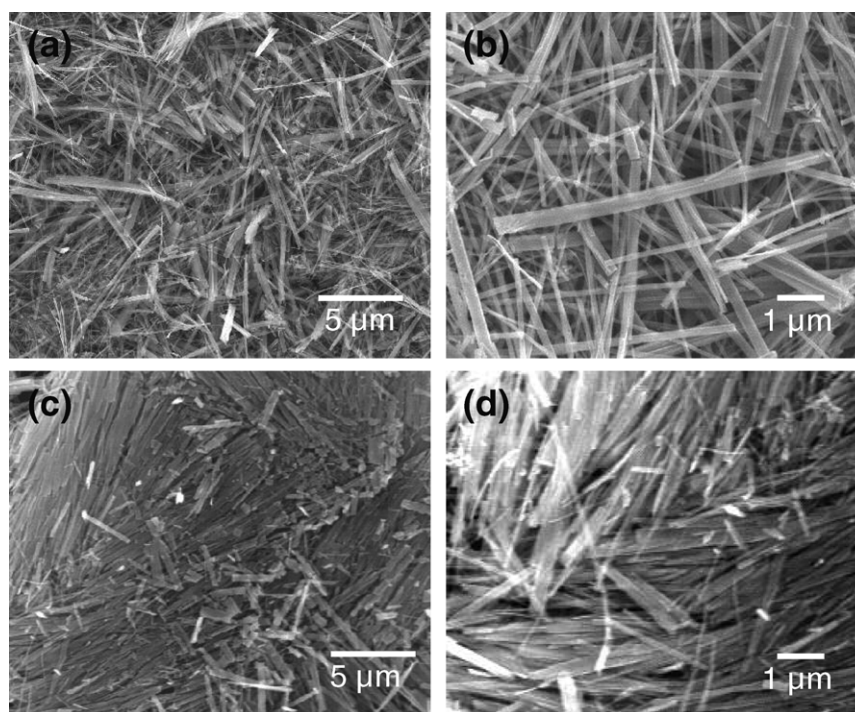


**Figure 2.** SEM images HCl ion exchange treated nanobelts for (a)–(b) 24 h and (c)–(d) 72 h.

suspension was stirred vigorously before vacuum-filtered through a filter paper. After the filtering was completed, a sheet of nanostructures was formed by sandwiching between a metal calender which was pressed and heated at 80 °C for approximately 2 h.

The scanning electron microscopy (SEM) characterization was carried out using a Philips XL30 FEG SEM with an accelerating voltage of 10 kV and attached Oxford Instrument energy dispersive x-ray (EDX). Carbon tape was used to adhere the sample which contributed to the carbon element being detected in the EDX spectra. The x-ray diffraction (XRD) characterization was done using a Philip x-ray diffractometer equipped with a graphite monochromator  $\text{Cu K}\alpha$  radiation, with  $\lambda$  wavelength of 1.541 Å at a scan rate of  $0.02^\circ \text{min}^{-1}$ . Fourier transform infrared spectroscopy (FTIR) measurements were carried out using Perkins Elmer spectrum 2000. The transmission electron microscopy (TEM) measurements were obtained using a JEOL-2100 with an accelerating voltage of 300 kV.  $I$ – $V$  measurements were obtained using a Keithley Semiconductor Characterization System 4200-SCS, with a sweep voltage from  $-3$  to  $3$  V and a compliance current of 0.1 A. The hydrogen-sensing measurements were obtained using a Keithley Semiconductor Characterization System 4200-SCS with a bias of 1 V with alternate dry air and  $\text{H}_2$  cycling.

### 3. Results and discussion

Hydrolysis and ion exchange of commercial  $\text{TiO}_2$  nanoparticles for growth of one-dimensional titanate and titania nanostructures are highly dependent on the concentration of the base (NaOH), duration of acid (HCl) washing as well as the calcination temperature employed. The effect of the

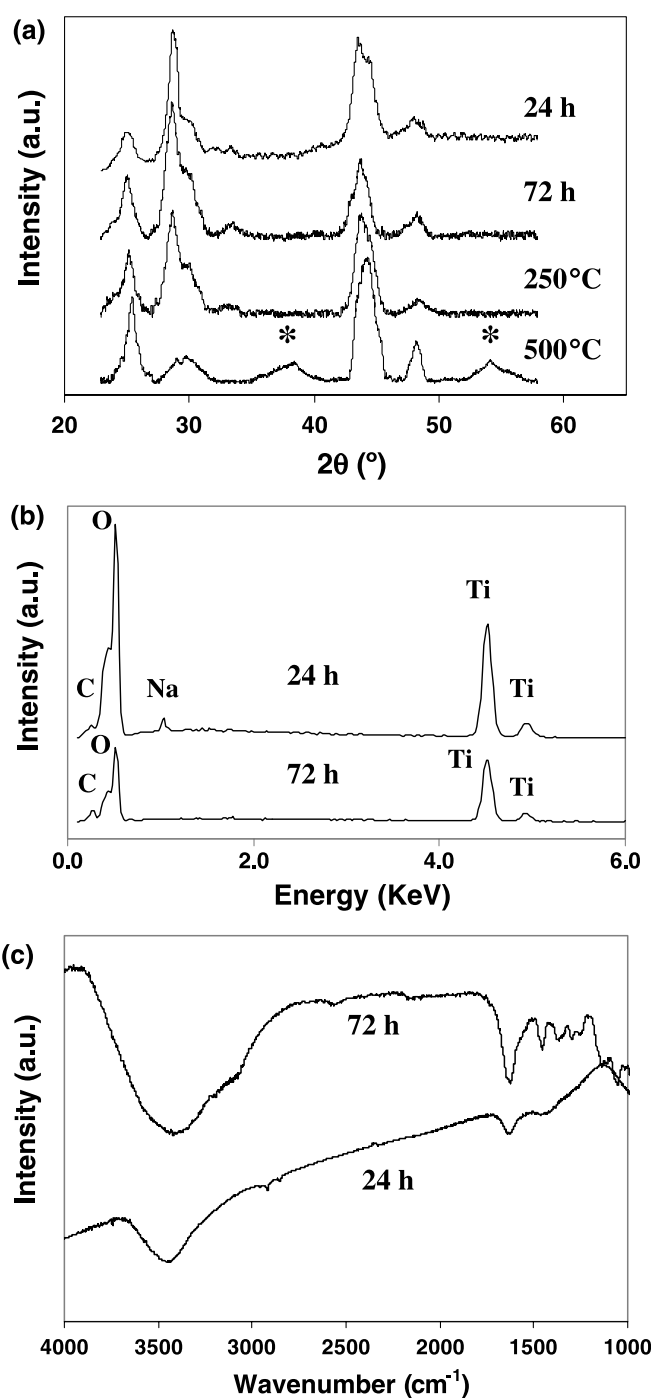
alkali hydrolysis is investigated with various concentration of NaOH. At concentration of 5M, the as-produced nanostructures are observed to be similar to the starting material,  $\text{TiO}_2$  nanoparticles (figures 1(a)–(b)). The produced nanoparticles retain their morphology and geometry with an average diameter of  $\sim 100$  nm. However, at a higher concentration of 10M, the nanostructures have distinctive belt-like morphologies as shown in figures 1(c)–(d). It is observed that only a small number of unreacted nanoparticles are present amongst the one-dimensional nanostructures. Typical widths of the one-dimensional nanostructures span from 50 nm to  $1 \mu\text{m}$  and the thicknesses are within the range 20 to 300 nm. The lengths of the nanobelts are greater than  $3 \mu\text{m}$  though longer lengths of up to  $20 \mu\text{m}$  are also observed. At even higher concentration of 15M, a mixture of nanobelts and highly agglomerated networks of two-dimensional thin nanosheets are produced (figures 1(e)–(f)). The nanobelts produced are shorter ( $2$ – $5 \mu\text{m}$ ) and sparsely distributed amongst the nanosheets. It has been known that the nanosheet is an unstable structure due to its high surface-to-volume ratio or high energy system. At specific reaction condition, there are two plausible ways in which the reconstruction of the nanosheets may occur transforming either the nanosheets into nanotube structures by folding up or nanobelts by epitaxial growth [16]. In our case, we observed that the nanobelts amongst the nanosheet-like structures may have aggregated through physical attraction due to the presence of high surface energy. It is postulated that the dangling bonds and large surface area of the two-dimensional nanosheet can strongly interact with their adjacent nanosheets via weak van der Waals forces leading to the formation of larger network of randomly aligned nanosheets.

The highest yield ( $\sim 95\%$ ) of nanobelts is attained when the concentration of NaOH is 10M. It is believed that when

the concentration of NaOH is relatively lower or higher than 10M, there is a subsequent decrease in the formation of one-dimensional nanobelts. Yuan and co-workers have reported similar observations [18]. Next, the effect of the HCl ion exchange acid washing duration time, 24 and 72 h, is investigated while keeping the rest of the reaction parameters constant. With a 24 h HCl ion exchange treatment, one-dimension nanostructures average width of 200 nm and length of 5  $\mu\text{m}$  are synthesized (figures 2(a)–(b)). On the other hand, longer HCl treatment time of 72 h produces bundles of shorter nanobelts (1–5  $\mu\text{m}$ ) possibly due to longer acid treatments which leads to breakages of the nanobelts (figures 2(c)–(d)). However, it is noted that both the samples with different HCl washing durations show no significant morphology changes, retaining nanobelt-like structures.

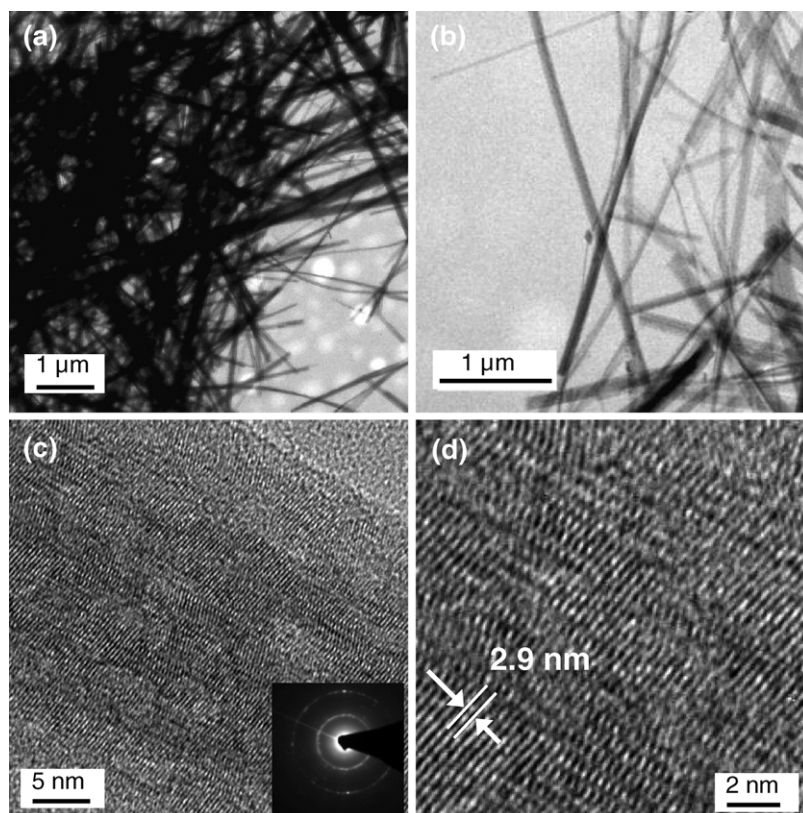
Figure 3(a) shows XRD spectra of samples with various reaction conditions. XRD spectrum obtained from the sample washed with 0.1M HCl for 24 h shows a relatively well-crystallized sodium titanate [19]. The chemical composition is confirmed using EDX which detected sodium, titanium, carbon and oxygen elements as shown in figure 3(b). After the hydrolysis process, protonated forms of sodium titanate are obtained with basically little  $\text{Na}_2\text{Ti}_3\text{O}_7$  transforming into hydrogen titanate ( $\text{H}_2\text{Ti}_3\text{O}_7$ ), i.e. the ion exchange of  $\text{Na}^+$  by  $\text{H}^+$  is not efficient with a short duration (24 h) of acid washing. Subsequently, XRD spectrum is obtained on the sample with prolonged acid washing of 72 h. EDX analysis as shown in figure 3(b) detected carbon, titanium and oxygen elements only. The absence of sodium may have suggested that the  $\text{Na}^+$  ions of the titanate nanobelts are effectively removed by longer acid leaching and neutralization process and the nanostructures are believed to have transformed into metastable titanate phase, hydrogen titanate compound [20]. According to the diffraction databases,  $\text{Na}_2\text{Ti}_3\text{O}_7$  (JCPDS 31-1329) and  $\text{H}_2\text{Ti}_3\text{O}_7$  (JCPDS 36-0654) have similar diffraction peak positions. It is reasonable to expect that such layered titanate structure should not be substantially affected in terms of its unit-cell dimension when a small alkali cation Na is replaced by H. However, it is noted that one of the diffraction peaks at  $\sim 43^\circ$  does not provide a satisfactory fit to the database. This may be due to the small dimensions of the nanostructures, surface defects or water incorporation in the matrix which may have modified the lattice parameters of the nanobelts. The effect of calcination temperature on the prolonged 72 h acid washed nanobelts is also studied using XRD. With a heat treatment up to 250  $^\circ\text{C}$ , the sample exhibits no significant changes in the diffraction pattern as the samples before heat treatment. However, when the sample is heat treated at 500  $^\circ\text{C}$ , it is observed that the first diffraction peak is shifted towards higher  $2\theta$  and becoming much sharper, a hybrid hydrogen titanate and onset anatase titania peaks (indicated by \*) are formed [20].

Figure 3(c) shows the FTIR spectra of HCl leaching for 24 and 72 h. Both spectra show peaks characteristic of the OH group at  $\sim 3400$  and  $1620\text{ cm}^{-1}$  [21] which indicates the presence of large amount of water and hydroxyl groups in the titanate nanobelts. The broader peaks centred at  $3400\text{ cm}^{-1}$  are O–H stretching vibrations while the peaks at  $1620\text{ cm}^{-1}$  are due to physically adsorbed water molecules H–O–H [21]. It is



**Figure 3.** (a) XRD spectra of nanobelts with acid washing for 24 and 72 h, post heat treatment of 250 and 500  $^\circ\text{C}$ . (b) EDX and (c) FTIR spectra of nanobelts with acid washing for 24 and 72 h.

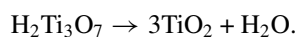
observed that the relative intensity of the O–H band increased with the HCl leaching duration which may suggest an increase of O–H crystal bonds due to the formation of hydrogen titanate. TEM image of figure 4(a) shows that the nanobelts are of high aspect ratio and non-hollow in structure. Figure 4(b) shows that with short duration of dispersion in ethanol, the nanobelts can be well dispersed and unagglomerated. The high resolution TEM image of figure 4(c) shows that the nanobelt has polycrystalline layered structure and is highly defective while figure 4(d) reveals interplanar spacing of 0.29 nm, which



**Figure 4.** (a)–(b) Low and (c)–(d) high resolution TEM images of the nanobelts. High resolution images show layered and highly defective structure.

corresponds to  $(-202)$  of sodium titanate [22]. It is noted that the interlayer spacing is highly dependent on the extent of proton exchange and water intercalation [23].

The formation mechanism of the nanobelts is via an alkali-hydrothermal process, which involves dissolution–crystallization process as shown in the schematic diagram (figure 5). Anatase  $\text{TiO}_2$  nanoparticle precursor is initially dissolved and hydrolysed into titanate under the hydrothermal reaction. During the alkali-hydrothermal reaction, the individual monomer of the crystalline precursor can be represented as the  $[\text{Ti}(\text{OH})_6]^{2-}$  octahedra. The unstable monomers react via oxolation/ololation to form sodium titanate and water. Subsequently, the sodium titanate nanobelts are washed with HCl to form hydrogen titanate and by-product sodium chloride. The  $\text{Na}^+$  cations of the octahedra titanium complexes can be substituted with  $\text{H}_3\text{O}^+$  cations by ion exchange when immersed in HCl for a sufficient time for complete conversion [24]. Anatase titania can then be obtained under heat treatment dehydration process of  $500^\circ\text{C}$ . The entire chemical processes that take place are as follows:



Thus, upon hydrolysis of titania particles using NaOH and adequate acid washing (by ion exchange), it was revealed that

as-synthesized nanostructures formed ‘Ti–O framework’—titanate and anatase titania. It is noted that the titanate and anatase titania have a common structural features, with both crystal lattices consisting of the octahedra sharing four edges and the zigzag chain-like structure (figure 5) [8]. These chains are joined together by sharing edges to form layers such that protons or  $\text{Na}^+$  ions which can be incorporated between the layers [8]. The distance between the layers is variable, which resulted in the high flexibility of these high aspect ratio nanostructures. In the reaction with the acid, the zigzag chain-like structural units of  $\text{TiO}_2$  nanobelts remain relatively unchanged other than lattice rotation and rearrangement of the  $[\text{TiO}_6]$  octahedra to form anatase lattice [8]. Thus, it is postulated that anatase titania phase formed on the basis of the parent titanate nanostructures. It is interesting to note that the produced titania and titanate nanostructures retain essentially the same morphology, even after intervention of different chemical processing steps, such as acid washing and high temperature treatment. This observation confirms that the titanate structural host motifs are easily intercalated with alkali metal with slight lattice rotation and rearrangement of crystal structures without modifying its final morphology.

Sheets of as-synthesized nanobelts are used for electrical and gas sensing measurements. Figure 6(a) shows the white nanobelts sheet made without any addition of binder or reinforcement chemicals. Cross-sectional SEM image of figure 6(b) shows that the nanobelts sheet has a thickness of  $\sim 15\ \mu\text{m}$ . In order to test the electrical resistivity of the metal-oxides in bulk form, the nanostructure sheet was cut into small

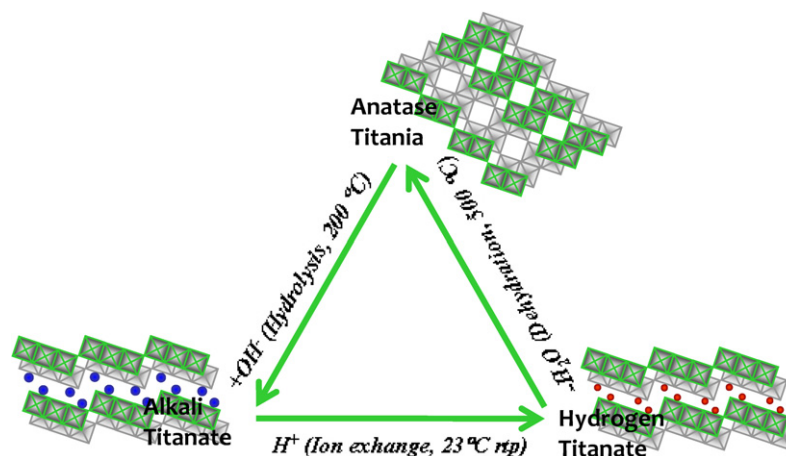


**Figure 5.** Schematic diagram of titania and titanate phase transitions by the wet-chemical reactions at various temperatures.

rectangular pieces which measured  $\sim 3 \times 5$  mm. This was placed on a clean  $\text{SiO}_2$  substrate and connected on both ends with silver paste. The schematic diagram of the fabricated sensor device is as shown in figure 7(a) inset. Figure 7(a) shows the  $I$ - $V$  characteristic curves of the nanobelts sheet under an applied voltage of  $-3$  to  $3$  V. A stable current reading clearly demonstrates that the nanostructures sheet provides a connecting Schottky electrical contact between pairs of silver electrodes. The contact properties depend on the difference of work functions between the electrodes and the semiconducting nanobelts. It is expected that in this case Schottky contact is established with the workfunction of Ag ( $4.26$  eV) greater than the workfunction of intrinsically n-type  $\text{TiO}_2$  ( $4.2$  eV) [25]. Figures 7(b) and (c) show the current response of the sensor at varying and same ppm  $\text{H}_2$  concentrations, respectively. The measurements were conducted at an operating temperature of  $300^\circ\text{C}$ . From the graphs, it is evident that the introduction of hydrogen causes the resistance of the sensor to reduce because of the injection of electrons onto the surface of the metal-oxide nanostructures, thereby improving the conductivity of the bulk sensing capabilities. The resistance increases as the concentration of  $\text{H}_2$  is varied from  $2500$  to  $1000$  ppm. The response time ( $90\%$  of  $R_{\text{air}} - R_{\text{gas}}$ ) is achieved within the first  $40$ – $50$  s while the recovery time is  $1.0$ – $1.2$  min. From figure 7(c), it was observed that the sensing response was rather stable and reversible. However, it is noted that over a prolonged gas sensing cycling at  $300^\circ\text{C}$ , the sensitivity of the material becomes unstable. It is well-known that single crystalline and epitaxial materials have excellent gas sensing stability characteristics [26]. In our case the as-synthesized nanobelts do not have high crystallinity quality (as evident from the structural TEM analysis) which may have an impact on the sensing properties. Anatase, the polymorph of titania has been reported to be of high sensitivity towards reducing gases such as hydrogen [27]. The magnitude of the gas response for sodium titanate sensor has been reported and it has been shown that Na inclusion had a negligible effect on the  $\text{H}_2$  sensing properties [28]. Here, we expect that our hybrid hydrogen titanate and anatase titania nanobelts have gas response properties of anatase titania without significant effect from the hydrogen titanate. In oxidizing atmosphere of

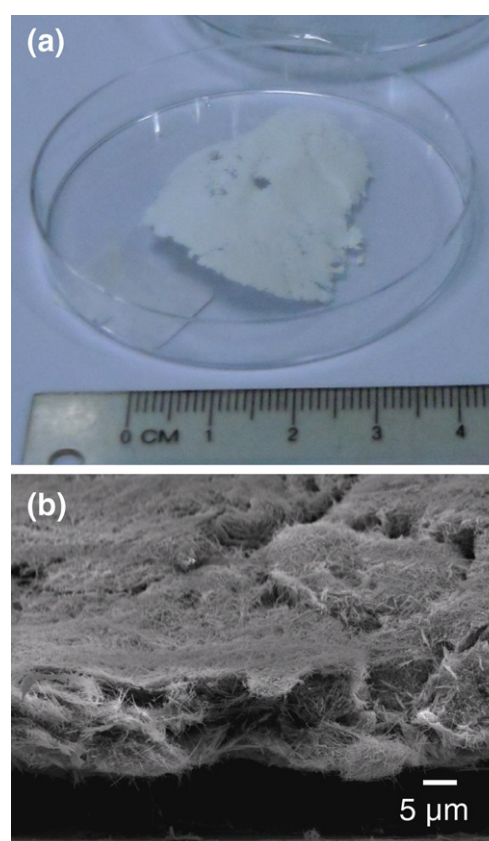


**Figure 6.** (a) Image of nanobelts sheet made without any addition of binder or reinforcement chemicals. (b) Cross-sectional SEM image of the nanobelts sheet.

$300^\circ\text{C}$ , ambient oxygen is adsorbed on the surface of nanobelts most likely with a negative charge. Subsequently, with the introduction of a reducing  $\text{H}_2$  gas, it reacts with the negatively charged surface oxygen and decreases the resistance by the injection of electron.

#### 4. Conclusion

Hydrolysis and ion exchange of titania particles via hydrothermal reaction at  $200^\circ\text{C}$  has produced one-dimensional

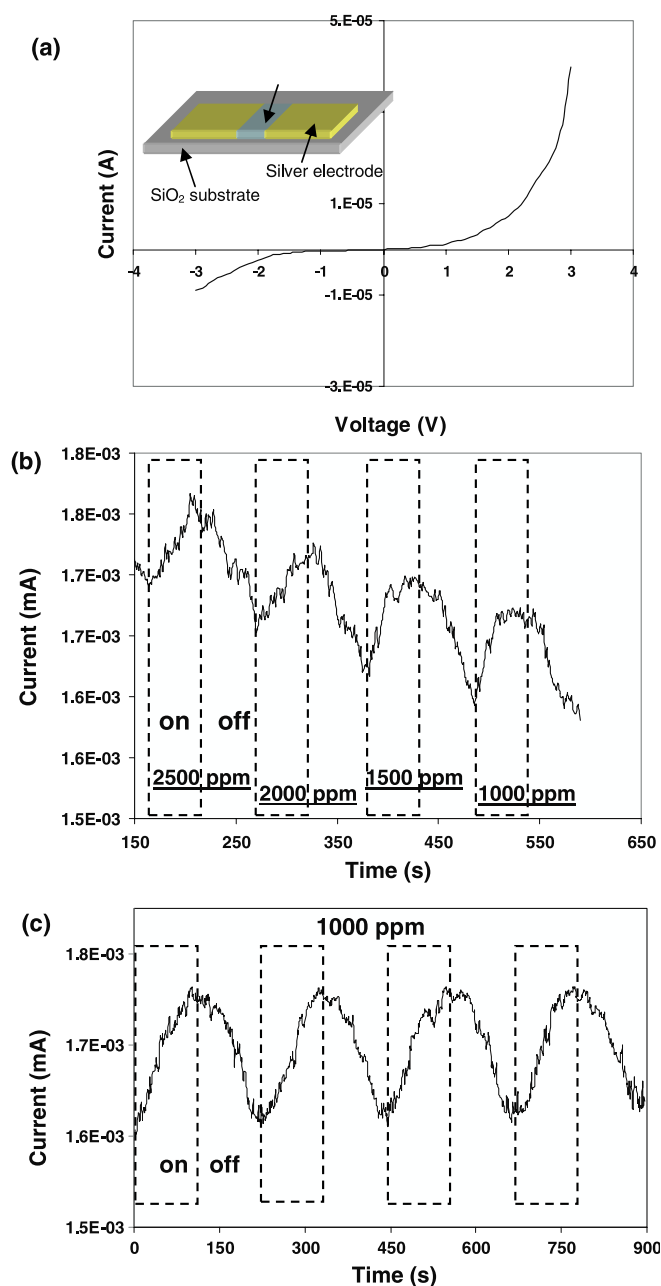


**Figure 7.** (a)  $I$ - $V$  characteristic curves of nanobelts sheet under an applied voltage of  $-3$  to  $3$  V. Inset: schematic diagram of the fabricated sensor. Current response of the sensor at (b) varying and (c) same ppm  $H_2$  concentration.

hybrid titanate and anatase titania nanobelts. The chemical composition is highly dependent on the concentration and duration of the NaOH and HCl processing, respectively. The product of the hydrolysis and ion exchange reaction, prior to HCl acid washing, is sodium titanate nanobelts. However, HCl leaching and neutralization process yield hydrogen titanate nanobelts which retain the nanobelt-like morphology. The nanobelts do not have high crystallinity quality due to the presence of alkali metal intercalated into Ti-O framework.

The sensing properties of titania nanobelts sheet is tested and exhibited response to  $H_2$  gas.

## Acknowledgment

This work is supported by the National University of Singapore (NUS) grant R-263-000-532-112.

## References

- [1] Hodos M, Horvath E, Haspel H, Kukovec A, Konya Z and Kiricsi I 2004 *Chem. Phys. Lett.* **399** 512-5
- [2] Mor G K, Shankar K, Paulose M, Varghese O K and Grimes C A 2005 *Nano Lett.* **5** 191-5
- [3] Kubota S, Johkura K, Asanuma K, Okouchi Y, Ogiwara N, Sasaki K and Kasuga T 2004 *J. Mater. Sci.: Mater. Med.* **15** 1031-5
- [4] Kavan L, Kalbac M, Zukalova M, Exnar I, Lorenzen V, Nesper R and Graetzel M 2004 *Chem. Mater.* **16** 477-85
- [5] Bavykin D V, Lapkin A A, Plucinski P K, Friedrich J M and Walsh F C 2005 *J. Phys. Chem. B* **109** 19422-7
- [6] Huang R, Chung F and Kelder E M 2006 *J. Electrochem. Soc.* **153** A1459-65
- [7] Dominko R, Baudrin E, Umek P, Arcon D, Gaberscek M and Jamnik J 2006 *Electrochem. Commun.* **8** 673-7
- [8] Zhu H Y, Lan Y, Gao X P, Ringer S P, Zheng Z F, Song D Y and Zhao J C 2005 *J. Am. Chem. Soc.* **127** 6730-6
- [9] Dagan G and Tomkiewicz M 1993 *J. Phys. Chem.* **97** 12651-5
- [10] Zhang S, Liu C Y, Liu Y, Zhang Z Y and Mao L 2009 *Mater. Lett.* **63** 127-9
- [11] Liu B and Aydil E S 2009 *J. Am. Chem. Soc.* **131** 3985-90
- [12] Qu J, Gao X P, Li G R, Jiang Q W and Yan T Y 2009 *J. Phys. Chem. C* **113** 3359-63
- [13] Seo M H, Yuasa M, Kida T, Huh J S, Shimano K and Yamazoe N 2009 *Sens. Actuators B* **137** 513-20
- [14] Jung H G, Oh S W, Ce J, Jayaprakash N and Sun Y K 2009 *Electrochem. Commun.* **11** 756-9
- [15] He B L, Dong B and Li H L 2007 *Electrochem. Commun.* **9** 425-30
- [16] Peng H R, Lia G C and Zhang Z K 2005 *Mater. Lett.* **59** 1142-5
- [17] Sun X, Chen X and Li Y 2002 *Inorg. Chem.* **41** 4996-8
- [18] Yuan Z Y and Su B L 2004 *Colloids Surf. A: Physicochem. Eng. Asp.* **241** 173-83
- [19] Kim G S, Godbole V P, Seo H K, Kim Y S and Shin H S 2006 *Electrochem. Commun.* **8** 471-4
- [20] Mao Y B, Kanungo M, Benny T H and Wong S S 2006 *J. Phys. Chem. B* **110** 702-10
- [21] Wang R, Hashimoto K, Fujishima A, Chikuni M, Kojima E A, Kitamura A, Shimohi-goshi M and Watanabe T 1998 *Adv. Mater.* **10** 135
- [22] Zarate R A, Fuentes S, Wiff J P, Fuenzalida V M and Cabrera A L 2007 *J. Phys. Chem. Solids* **68** 628-37
- [23] He M, Feng X, Lu X H, Ji X Y, Liu C, Bao N Z and Xie J W 2004 *J. Mater. Sci.* **39** 3745-50
- [24] Wei M, Konishi Y, Zhou H, Sugihara H and Arakawa H 2004 *Chem. Phys. Lett.* **400** 231-4
- [25] Hou X G, Huang M D, Wu X L and Liu A D 2009 *Chem. Eng. J.* **146** 42-8
- [26] Korotcenkov G 2008 *Mater. Sci. Eng. R* **61** 1-39
- [27] Birkefeld L D, Azad A M and Akbar S A 1992 *J. Am. Ceram. Soc.* **75** 2964-8
- [28] Kim H S, Moon W T, Jun Y K and Hong S H 2006 *Sensors Actuators B* **120** 63-8